ELSEVIER

Polymer 41 (2000) 7531–7538

polymer

Packing effect on oxygen diffusion in latex films; a photon transmission and fluorescence study

Ö. Pekcan*, Ş. Uğur

Istanbul Technical University, Department of Physics 80626, Maslak, Istanbul, Turkey

Received 22 March 1999; received in revised form 13 October 1999; accepted 21 January 2000

Abstract

Photon transmission (PT) and steady state fluorescence (SSF) methods were used to study latex film formation and oxygen diffusion processes, respectively. Films with different latex content were prepared separately by annealing pyrene (P) labeled poly(methyl methacrylate) (PMMA) particles above the glass transition temperature. Annealing was performed at three different temperatures. The transmitted photon intensity from these films decreased as the latex content is increased. It is observed that as the latex particles are packed more voids or cracks are formed in the films. Absorption coefficients, κ, were measured for each film sample annealed at different temperatures. The SSF method was employed to monitor oxygen diffusion into these latex films. Diffusion coefficients, *D*, of oxygen were determined for various films of different thicknesses and at different annealing temperatures and were found to increase from 0.45×10^{-10} to 73×10^{-10} cm^2 s^{-1} by increasing the film thickness from 10 to 100 μm. No temperature effect was observed on the diffusion coefficient, *D*, values.

Keywords: Photon transmission; Latex content; Diffusion coefficients

1. Introduction

In the last two decades latex film formation in coating industries has received extensive attention. In latex coatings the polymer chains are confined in particles which must coalesce during solvent evaporation and subsequent aging to form a mechanically rigid, protective film. Such films are more permeable to moisture than the solvent-based coatings in which polymer chains are entangled and fully interpenetrating as they are applied to the surface. The quality of coalescence of latex-based coatings has a dramatic effect on final film properties.

The term “latex film” normally refers to a film formed from soft particles where the forces accompanying the evaporation of water are sufficient to compress and deform the particles into a transparent, void-free film [1–4]. However, hard latex particles remain essentially discrete and undeformed during the drying process. Film formation from these dispersions can occur in several stages. In both cases, the first stage corresponds to the wet initial state. Evaporation of the solvent leads to the second stage, in which the particles form a close packed array, and if the particles are soft they are deformed to polyhedrons. Hard latex, however, stays undeformed at this stage. Annealing of soft particles cause diffusion across particle–particle boundaries which allows the film to be a homogeneous continuous material. In the annealing of the hard latex system, however, deformation of particles first leads to void closure [2] and after the voids disappear diffusion across particle–particle boundary starts, i.e. the mechanical properties of hard latex films can be evolved by annealing, after all the solvent has evaporated and all the voids have disappeared. After the void closure process is completed, the mechanism of film formation, by the annealing of hard latex films is known as interdiffusion of the polymer chains across the polymer–polymer interfaces [5–8].

The process of interparticle polymer diffusion has been studied by direct nonradiative energy transfer (DET) using fluorescence decay measurements in conjunction with particles labeled with the appropriate donor and acceptor chromopher [9–11]. This transient fluorescence technique has been used to examine a latex film formation of 1 μm diameter high-*T* PMMA particles [10,11] and of 100 nm diameter low-*T* poly(butyl methacrylate) (PBMA) particles [9]. All these studies indicate that in the particular systems examined, annealing the films above T_g leads to the polymer interdiffusion at the particle–particle junction as the particle interfaces heals. Mazur [2] has written an extensive review on the coalescence of polymer particles, in which he mainly

---

* Corresponding author. Tel.: + 90-212-285-3213; fax: + 90-212-285-6366.

PII: S0032-3861(00)00079-3

discussed the neck growth mechanism and its several geometrical approximations before interdiffusion of the polymer chain takes place. DET and the steady state fluorescence technique have been used to study interdiffusion processes at the particle–particle junction during film formation by high-*T* PMMA latex particles [12–14]. Recently photon transmission technique was developed in this laboratory for studying latex film formation for both soft and hard latex particles [15–17].

Most of the photophysical and chemical reactions taking place in polymers occur as a result of the mass diffusion of the reactants. Knowledge of the diffusion coefficient of these reactants into the polymeric system is of prime importance in the development of materials of desired properties. Oxygen is one of the most important reactants to be considered in the diffusion phenomenon. The control of the diffusion of oxygen is of particular importance in the design of polymeric membranes for separation processes in the production of films for packing industries, and in the development of biocompactible materials.

The usual procedures used to measure the diffusion coefficients of gases through polymeric system are based upon measurements of the amount of gas, which permeates a given area of polymer in a given time. In addition to this direct method of determination, depending upon the properties of the gases being investigated there are also indirect methods that are based on the quenching or bleaching action of these gases on the molecular probes imbedded uniformly in the polymer. The diffusion coefficient of oxygen into PMMA was determined by the quenching of the phosphorescence of phenanthrene added into the polymer [18]. Barker has utilized the bleaching action of oxygen on color centers produced by the electron beam irradiation of polycarbonate and PMMA by following optically the moving boundary [19]. The quenching of the fluorescence of naphthalene in PMMA was studied by oxygen in thin films after the displacement of nitrogen atmosphere over the sample by oxygen [20]. ESR spectroscopy method was used for measuring oxygen diffusion coefficient in PMMA spheres [21]. Every technique mentioned above carries some inherent advantage and disadvantages.

In this work various latex films formed from pyrene labeled hard latex particles with different latex content were annealed for 60 min time intervals at 180, 200 and 220°C. Transmitted photon intensities, I_{tr} from annealed latex films were measured by UV–visible (UV–Vis) technique to study the packing effect. It is observed that I_{tr} obeyed the Beer–Lambert law by decreasing as the latex content was increased. Steady state fluorescence technique was used to study oxygen diffusion into these annealed polymeric latex films. The time drive mode of SSF spectrometer was employed to monitor the intensity change of excited P during oxygen penetration into latex films. A model was developed for the low quenching efficiency to measure oxygen diffusion coefficient, *D*.

2. Experimental

Pyrene (P)-labeled PMMA-PIB polymer particles sterically stabilized by poly(iso butylene) (PIB) were prepared separately in a two-step process which is reported elsewhere [16]. These spherical particles ranged in diameter of 1–3 μm. Glass transition temperatures of these particles are found to be around 110°C. These particles are made up of polymers with a molecular weight of $M_{\mathrm{w}} \cong 2.15 \times 10^5$ with the polydispersity of 1.49. A combination of ^{1}H NMR and UV-V analysis indicated that these particles contain 6 mol% PIB and 0.037 mmol P groups per gram of polymer. (These particles were prepared in Prof. M.A. Winnik's Laboratory in Toronto). Latex film preparation was carried out in the following manner. The pyrene labeled particles were dispersed in heptane in a test tube. After complete mixing, six different film samples were prepared by placing different number of drops on a glass plates with the size of $0.8 \times 2.5\ \mathrm{cm}^2$. The heptane was allowed to evaporate. Then the films were annealed sequentially at 180, 200 and 220°C temperatures for 60 min time intervals. During annealing, the temperature was maintained within ±2°C. Samples were weighted before and after film casting to determine the latex contents and thicknesses of the films. These values are summarized in Table 2. The average particle size was taken as 2 μm to calculate the thickness of the film.

The UV-V experiments for the latex film formation were carried out with the model Lambda 2S UV–Visible spectrometer of Perkin–Elmer and the transmittance of the films was detected at 400 nm. In situ fluorescence measurements for oxygen diffusion experiments were performed by placing films in a round quartz tube filled with nitrogen, in a Perkin–Elmer Model LS-50 fluorescence spectrometer. Slit widths were kept at 8 nm. Pyrene was excited with 345 nm at room temperature. Film samples were illuminated only during the actual fluorescence measurements and, at all other times, were shielded from the light source. O_2 diffusion experiments were performed for each film sample at room temperature and in all experiments maximum peak at 395 nm were used for the pyrene intensity (*I*) measurements. The change in pyrene intensity, *I* was monitored against time, after the quartz tube was open to the air for O_2 diffusion experiments.

3. Theoretical considerations

3.1. Turbidity of latex films

When the latex film is formed and annealed it goes from the turbid to the transparent state. Usually the turbidity of a medium is created by the scattering of light. If the intensity of incident light is I_0, and on passage of the light through a medium of thickness *d* the incident intensity is reduced to I_{tr}

as a result of scattering then the turbidity of the medium is determined by the following equation

$$\frac{I_{\mathrm{tr}}}{I_0} = \exp(-\tau d) \tag{1}$$

where turbidity, τ, is defined as the fraction of the primary light beam scattered in all directions on passage through a medium with thickness of 1 cm i.e.

$$\tau = \ln\left(\frac{I_{\mathrm{tr}}}{I_0}\right) \tag{2}$$

The expression I_{tr}/I_0 has been known as the light transmission or relative transparency. In general turbidity is given by $\tau = (\epsilon + \kappa)c$, where ϵ and c are the molar absorption coefficient and the molar concentration, κ the imaginary absorption coefficient. ϵ usually depends on the wavelength of the light, being observed, temperature and nature of the medium. ϵ presents the true absorption of light i.e. when light is absorbed by a system its energy is transformed into thermal energy. The molar absorption coefficient, ϵ, does not include the size of the particles if they exist in the medium. It is known that the size of the colloidal particles affects light absorption indirectly through either light scattering or reflection. In general light is scattered only when its wavelength is greater than the size of a particle in the medium. If the wavelength of the light is much smaller than the particle diameter, light is reflected. When the size of particles becomes considerably greater than λ, light is no longer scattered but reflected, regardless of the light wavelength. If the particles are too large, light reflection from them increases which causes the reduction of the intensity of scattered light. The fact is that, as a result of light scattering, the white light, which passes through a medium, still loses some radiation in the short wavelength region, which is not the true absorption. Such absorption is known as the imaginary absorption, which is identified with κ, which is a function of the particle size. If $\epsilon = 0$ the system has no true absorption i.e. the system is white.

In our experiments the wavelength of the light is 10 times smaller than the latex particle and is comparable to the void size. In our case it is believed that the latex film reflects light but does not make true absorption. A decrease in the transmitted light intensity most probably caused by the imaginary absorption occurred in the latex system. In fact, on the annealing of latex films around the melting temperature of PMMA, no traces of voids can be seen, as a result most of the light is reflected by the cracks, which can especially exist in the thicker films. The sizes of these cracks can be even larger than the size of the latex particles, which are formed after viscous flow i.e. void closure process.

3.2. Fluorescence quenching by oxygen

When samples containing fluorescent probes are exposed to air or their solutions saturated with oxygen, the fluorescence intensities of the samples decrease and the rates of fluorescence decay increase. These phenomena are due to oxygen quenching of the probe's excited state. The mechanism of quenching involves a sequence of spin allowed internal conversion processes, which takes place within a weakly associated encounter complex between the probe and oxygen. The product is either a singlet ground state or an excited triplet species [22].

Data generated from oxygen quenching studies on small molecules in homogeneous solution are usually analyzed using the Stern–Volmer relation (Eq. (3)), provided that the oxygen concentration $[\mathrm{O}_2]$ is not too high [23].

$$\frac{I_0}{I} = 1 + k_{\mathrm{q}}\tau_0[\mathrm{O}_2] \tag{3}$$

In this equation, I and I_0 are the fluorescence intensities in the presence and absence of oxygen, respectively, k_{q} the bimolecular quenching rate constant and τ_0 the fluorescence lifetime in the absence of O_2. This equation requires that the decay of fluorescence is single exponential and, moreover, that quenching interactions occur with a unique rate constant k_{q}. From the slope of a plot of I_0/I versus $[\mathrm{O}_2]$, k_{q} can be determined provided that τ_0 is known. Diffusion coefficients related to the quenching events can be calculated from the time-independent Smoluchowski–Einstein [23] equation

$$k_{\mathrm{q}} = \frac{4\pi \mathrm{N_A}(D_{\mathrm{p}} + D_{\mathrm{q}})pR}{1000} \tag{4}$$

where D_{p} and D_{q} are diffusion coefficients of the excited probe and quencher, respectively, p the quenching probability per collision, R the sum of the collision radii ($R_{\mathrm{p}} + R_{\mathrm{q}}$), and $\mathrm{N_A}$ the Avagadro number. Eqs. (3) and (4) can also be applied to the case of quenching of polymer-bound excited states in glass as long as the fluorescence decay is exponential and k_{q} is single-valued. A simplifying factor in the interpretation of k_{q} is the general assumption that $D_{\mathrm{p}} \ll D_{\mathrm{q}}$ when the probe is covalently attached to a polymer. For quenchers as small as molecular oxygen, such an assumption would not be unwarranted. On the time scale of fluorescence the overall translational diffusion coefficient of the polymer coil is usually not important; the relevant diffusion coefficient is that for the motion of individual chain segments.

3.3. Diffusion in plane sheet

When Fick's second law of diffusion is applied to plane sheet and solved by assuming a constant diffusion coefficient, the following equation is obtained for concentration changes in time [24]

$$\frac{C}{C_0} = \frac{x}{d} + \frac{2}{\pi}\sum_{n=1}^{\infty}\frac{\cos n\pi}{n}\sin\frac{n\pi x}{d}\exp\left(-\frac{Dn^2\pi^2 t}{d^2}\right) \tag{5}$$

where d is the thickness of the slab, D the diffusion coefficient of the diffusant, and C_0 and C the concentration of the diffusant at time zero and t, respectively. x corresponds to the distance at which C is measured. We can replace the concentration terms directly with the amount of diffusant by using Eq. (6).

$$M = \int_v C\,\mathrm{d}V \tag{6}$$

when Eq. (6) is considered for a plane volume element and substituted in Eq. (5), the following solution is obtained [24]:

$$\frac{M_t}{M_\infty} = 1 - \frac{8}{\pi^2}\sum_{n=0}^{\infty}\frac{1}{(2n+1)^2}\exp\left(-\frac{D(2n+1)^2\pi^2 t}{d^2}\right) \tag{7}$$

where M_t and M_∞ represent the amounts of diffusant entering the plane sheet at time t and infinity, respectively.

4. Results and discussion

4.1. Latex film formation

The UV-V transmission curves for the film samples of various thicknesses annealed for 60 min at 180, 200 and 220°C are shown in Fig. 1a–c, respectively. Transmitted photon intensities are plotted versus film thickness, d, in Fig. 2a–c for six different latex film samples annealed at 180, 200 and 220°C where it is seen that I_{tr} decreased as the film thickness increased which obey Beer–Lambert Law as

$$I_{\mathrm{tr}} = I_0 \exp(-\kappa d) \tag{8}$$

here κ is the imaginary absorption coefficient and d the film thickness. The data in Fig. 2 are fitted to the logarithmic form of Eq. (8) and plotted in Fig. 3. The slopes of the linear relations in Fig. 3a–c produced κ values for films annealed at 180, 200 and 220°C temperatures. These values are listed in Table 1 where it is seen that as the annealing temperature is increased, the κ value decreased, which indicates that films become more transparent at higher annealing temperatures.

4.2. Oxygen diffusion

In Fig. 4 pyrene intensity, I curves are presented against time for films having different thicknesses, annealed at 180°C for 60 min time intervals and exposed to oxygen. It is seen that as the time is increased, I decreased due to oxygen absorption by latex films, as a result excited P molecules are quenched by oxygen according to Eq. (3). In order to interpret the above findings Eq. (3) can be expanded in a series for low quenching efficiency i.e. $k_q t_0[O_2] \ll 1$ which then produces the following useful result

$$I \approx I_0(1 - k_q \tau_0[O_2]) \tag{9}$$

During O_2 diffusion into the latex films, P molecules are quenched in the volume which is occupied by O_2 molecules at time, t. Then P intensity at time t can be represented by the

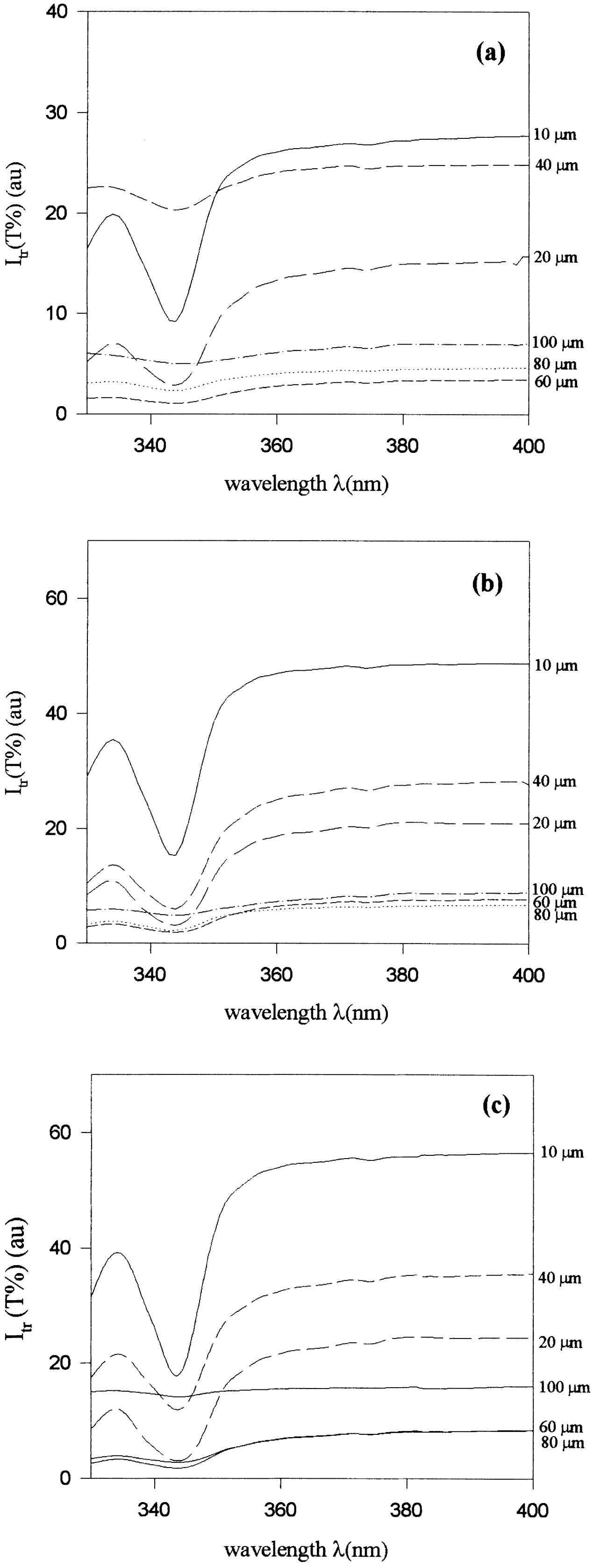

Fig. 1. UVV transmission curves for the latex films in various thicknesses annealed for 60 min at: (a) 180°C; (b) 200°C; (c) 220°C. Numbers on each curve indicate the film thicknesses.

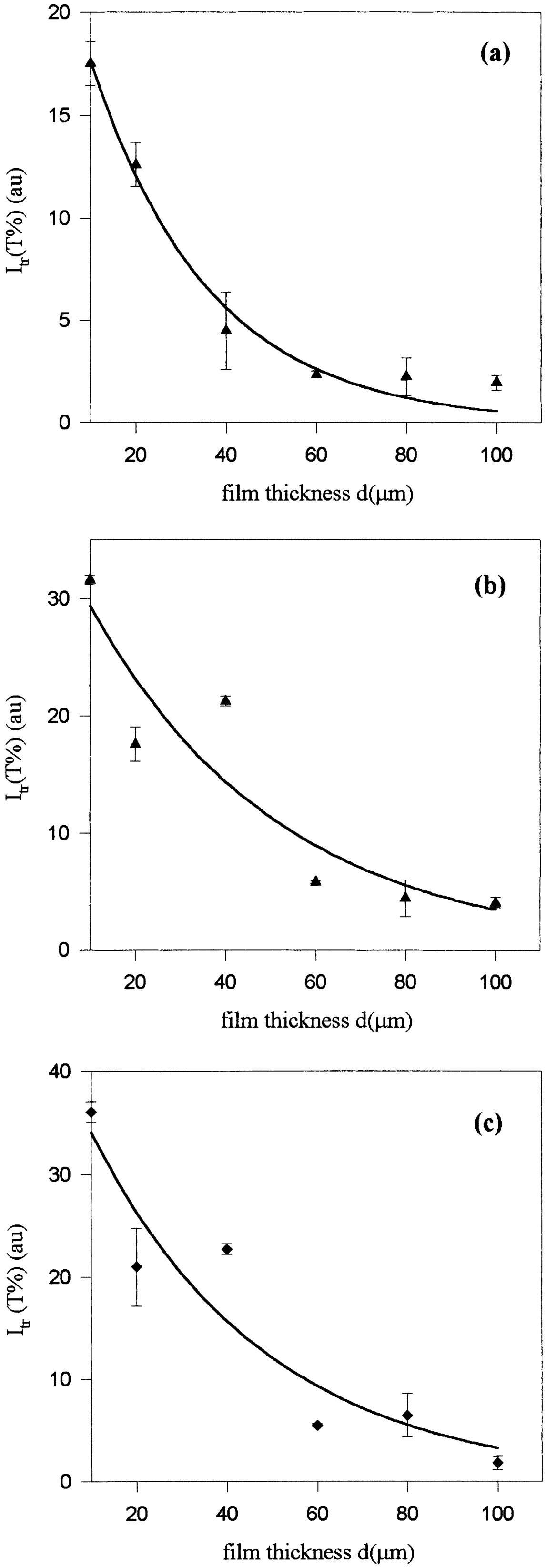

Fig. 2. Plot of transmitted photon intensity, I_{tr} against film thickness, d for the latex films annealed for 60 min time interval at: (a) 180°C; (b) 200°C; (c) 220°C.

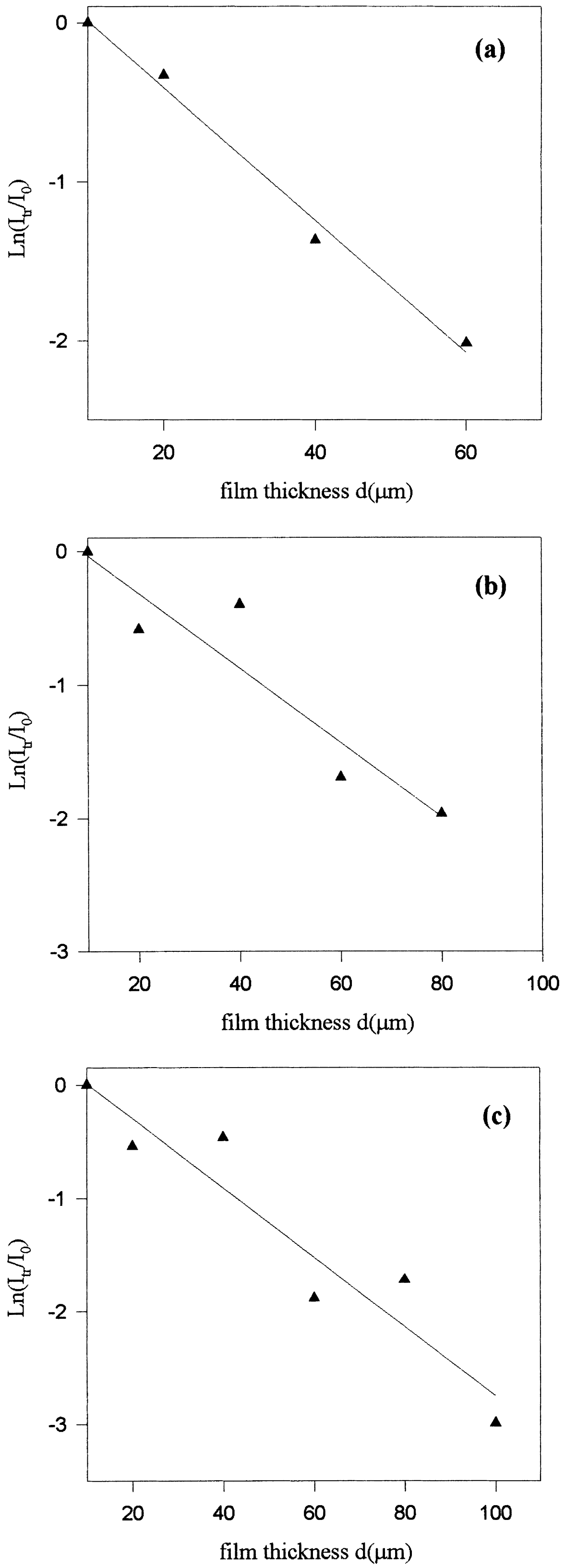

Fig. 3. The fit of the data in Fig. 2 according to logarithmic form of Eq. (8). The slopes of the curves produced the imaginary absorption coefficient, κ for the film samples annealed at: (a) 180°C; (b) 200°C; (c) 220°C.

Table 1
Experimentally obtained absorption coefficients

Annealing temperature T (°C)	Absorption coefficient κ (cm^{-1})
180	417
200	279
220	306

volume integration of Eq. (9) as

$$I_t = \frac{\int I \, dv}{\int dv} = I_0 - \frac{k_q \tau_0 I_0}{V} \int dv[O_2] \tag{10}$$

where dv and V are the differential and total volume of the latex film. Performing the integration the following relation is obtained

$$I_t = I_0\left(1 - k_q \frac{\tau_0}{V} O_2(t)\right) \tag{11}$$

where $O_2(t) = \int dv[O_2]$ is the amount of oxygen molecules that diffuse into the latex film at time t. Here $O_2(t)$ corresponds to M_t in Eq. (7). Combining Eq. (7) for oxygen with Eq. (11) the following useful relation is obtained to interpret the diffusion curves in Fig. 4

$$\frac{I_t}{I_0} = 1 - C + \frac{8C}{\pi^2} \exp\left(-\frac{D\pi^2 t}{d^2}\right) \tag{12}$$

where d is the film thickness and D the oxygen diffusion coefficient and $C = (k_q \tau_0 O_2(\infty))/V$. Here $O_2(\infty)$ is the amount of oxygen molecules that diffuse into the latex film at time infinity. Eq. (12) is fitted to the digitized and normalized P intensity data in Fig. 5a–c for the latex films at various film thickness annealed at 180°C. Similar fittings are done for the other film samples annealed at 200 and 220°C temperatures and k_q and D values are obtained. The measured D values are listed in Table 2. It is observed that diffusion coefficients of oxygen, D, are found to be dependent on the thickness of latex films. In Fig. 6 D values versus d were plotted for all film samples where quadratic dependence between these parameters are observed. The data in Fig. 6 obeyed the following relation

$$D = \alpha d^2 \tag{13}$$

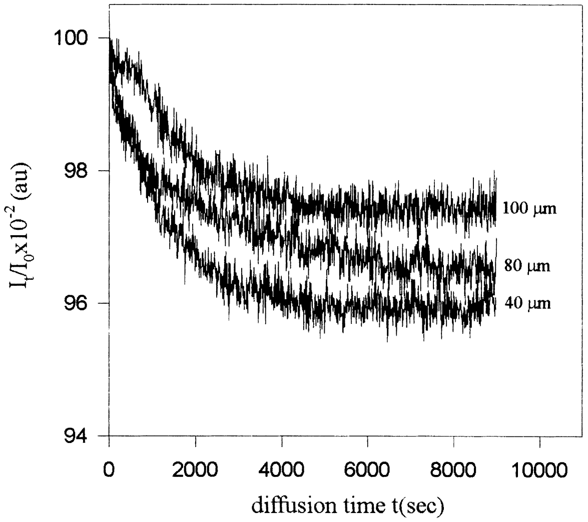

Fig. 4. The time behavior of the pyrene, P fluorescence intensity, I during oxygen diffusion into the latex films having different thicknesses annealed at 180°C temperature. Numbers on each curves indicate the film thickness.

which is presented in Fig. 7 for all the film samples annealed at 180, 200 and 220°C.

Here Fig. 7 and Eq. (13) predict that O_2 diffuses into the thicker latex films much faster than it does into the thin films. Fig. 2 suggests that thicker films are formed much looser than thin films. In other words thicker films have more pores and cracks which scatter more light than thin films. Naturally oxygen can diffuse much faster into the looser, thicker films than in thin films.

When the pyrene diffusion in the latex film is omitted and $p = 1$ is taken then Eq. (4) becomes

$$k_q = \frac{4\pi N_A D_m R}{1000} \tag{14}$$

Here D_m is the as mutual diffusion coefficient which can now be assumed to be the diffusion coefficient of O_2 in the latex film since k_q is known. If R is taken as the radius of pyrene then the averaged D_m values are found and listed in Table 1 for the latex films having different thickness and annealed at 180, 200 and 220°C. Here it has to be noticed that the penetration of oxygen molecules into the latex film is much slower than the diffusion of oxygen in the latex film.

Table 2
Experimentally obtained diffusion (D) and mutual diffusion (D_m) coefficients

Film thickness d (μm)	Diffusion coefficients of oxygen[a] $D \times 10^{-10}$ (cm^2 s^{-1})			Mutual diffusion coefficient $D_m \times 10^{-6}$ (cm^2 s^{-1})		
	180°C	200°C	220°C	180°C	200°C	220°C
10	0.45 ± 0.04	0.5 ± 0.03	0.52 ± 0.02	5.95 ± 2.64	2.73 ± 0.70	3.63 ± 2.43
20	2.02 ± 0.04	3.84 ± 0.07	3.16 ± 0.39	6.17 ± 1.88	2.11 ± 0.45	2.37 ± 0.83
40	9.28 ± 2.18	10.9 ± 0.54	17.34 ± 6.28	4.0 ± 1.29	6.95 ± 0.45	2.57 ± 0.52
60	24.29 ± 2.48	18.7 ± 0.83	26.32 ± 3.51	4.16 ± 2.08	3.39 ± 1.52	5.26 ± 0.84
80	37.55 ± 6.10	51.4 ± 8.88	47.61 ± 3.66	8.29 ± 0.26	4.42 ± 0.88	5.29 ± 0.58
100	67.03 ± 2.43	49.5 ± 3.54	72.98 ± 7.91	2.01 ± 0.26	7.36 ± 0.60	4.30 ± 0.50

[a] Diffusion coefficients of oxygen are obtained by fitting the data in Fig. 5a–c to Eq. (12) for the latex films at various thicknesses.

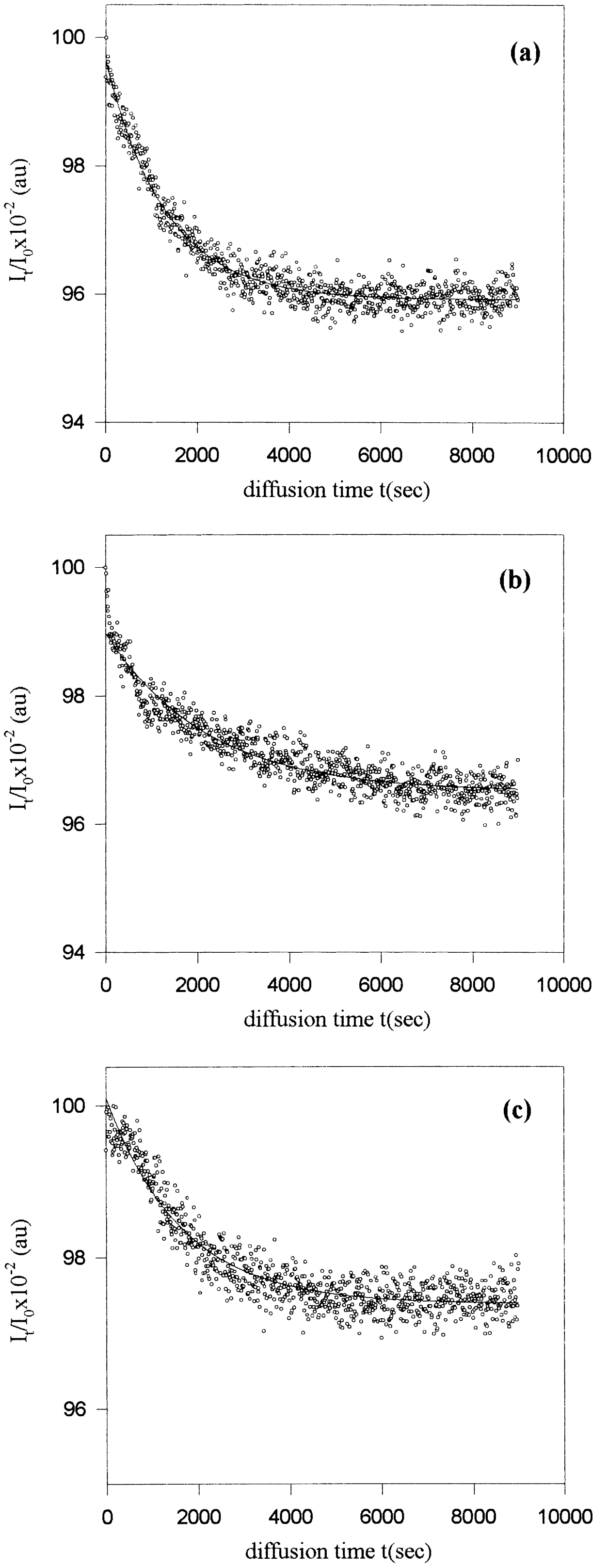

Fig. 5. Fit to the data in Fig. 4 according to Eq. (12) for the latex films having: (a) 40 μm; (b) 80 μm; (c) 100 μm thicknesses.

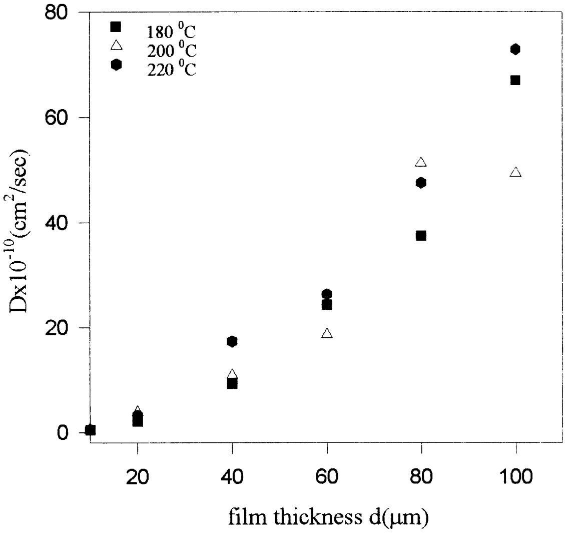

Fig. 6. Plot of the diffusion coefficients, *D* versus film thickness, *d* for the films annealed at 180, 200 and 220°C.

The plot of D_m versus d in Fig. 8 indicates that D_m is independent of packing (thickness) in latex films i.e. once the O_2 penetrates into the film then it moves around independent of the material structure.

5. Conclusions

This work has shown that simple SSF technique can be used to measure the diffusion coefficient of oxygen molecules into polymeric films quite accurately and the UV–Vis method predicts that the packing effect of latex particles on oxygen diffusion is crucial. Here it is shown

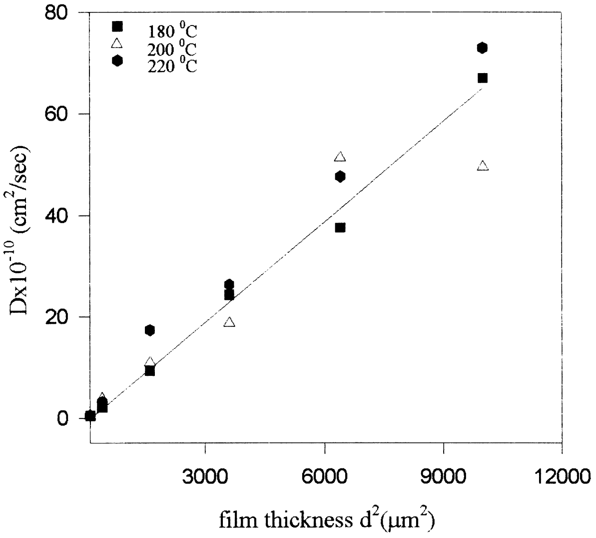

Fig. 7. Plot of *D* values against d^2.

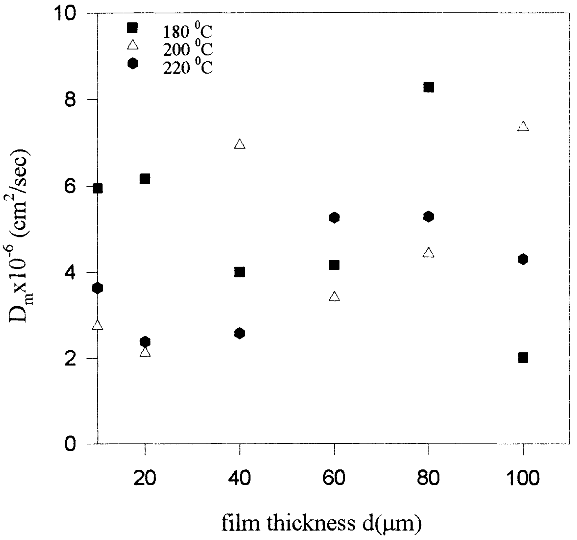

Fig. 8. Plot of D_m values against *d*.

that the turbidity of latex films is related to the cracks created during viscous flow and void closure process in thicker films by annealing them around melting temperature. These cracks are some imperfections created due to high packing of latex particles in thicker films, which can cause faster diffusion of oxygen molecules into these films. In other words cracks increase the surface area against oxygen molecules penetrating into the films as a result of oxygen diffusion into the thicker films much faster than thinner films. In this sense Eq. (13) can be written by including the number of cracks per unit volume, *n*, which then offers one to modify Eq. (7) for the Fickian diffusion in plane sheet for porous media. On the other hand, the results in Fig. 8 suggest that the diffusion of oxygen molecules in the bulk PMMA are not affected by the size and the structure of the latex films. In other words D_m values give information only on local environment.

References

[1] Sperry PR, Snyder BS, O'Down ML, Lesko PM. Langmuir 1994;10:2619.
[2] Mazur S. Coalescence of polymer particles. In: Maukis M, Rosenweig V, editors. Polymer powder technology, New York: Wiley, 1996.
[3] Keddie, JL, Meredith, P, Jones, RAL, Ronald, AM. Proceeding of the ACS, Chicago, 1995.
[4] Mackenzie JK, Shuttleworth R. Proc Phys Soc 1949;62:838.
[5] Kausch HH, Tirrell M. Annu Rev Mater Sci 1989;19:341.
[6] Hahn K, ley G, Schuller H, Oberthur R. Coll Polym Sci 1988;66:631.
[7] Yoo JN, Sperling LH, Glinka CJ, Klein A. Macromolecules 1990;23:3962.
[8] Kim KD, Sperling LH, Klein A. Macromolecules 1993;26:4624.
[9] Wang Y, Zhao CL, Winnik MA. J Chem Phys 1991;95:2143.
[10] Zhao CL, Wang Y, Hrus Z, Winnik MA. Macromolecules 1990;23:4082.
[11] Pekcan Ö, Winnik MA, Croucher MD. Macromolecules 1990;23:2673.
[12] Canpolat M, Pekcan Ö. Polymer 1995;36:2025.
[13] Pekcan Ö, Canpolat M. J Appl Polym Sci 1996;59:277.
[14] Canpolat M, Pekcan Ö. Polymer 1997;38:2595.
[15] Pekcan Ö, Arda E, Kesenci K, Piþkin E. J Appl Polym Sci 1998;68:1257.
[16] Pekcan Ö, Arda E. J Appl Polym Sci 1998;70:339.
[17] Pekcan Ö, Arda E. Polym Int 1998;47:231.
[18] Shaw G. Trans Faraday Soc 1967;63:2181.
[19] Barker RE. J Polym Sci 1962;58:553.
[20] Mac Callum JR, Rudkin AL. Eur Polym J 1978;14:655.
[21] Kaptan Y, Pekcan Ö, Arca E, Güven O. J Appl Polym Sci 1989;37:2577.
[22] Birks JB. Organic molecular photophysics. New York: Wiley, 1975.
[23] Rice SA. Diffusion-limited reactions. In: Bamford CH, Tipper CFH, Compton RG, editors. Comprehensive chemical kinetics, Amsterdam: Elsevier, 1985.
[24] Crank J. The mathematics of diffusion. London: Oxford University Press, 1970.